WIRELESS COMMUNICATIONS AND MOBILE COMPUTING
Wirel. Commun. Mob. Comput. 2011; **11**:1551–1563
Published online 3 November 2011 in Wiley Online Library (wileyonlinelibrary.com). DOI: 10.1002/wcm.1212

SPECIAL ISSUE PAPER

Recent advances in single-carrier distributed antenna network

Fumiyuki Adachi*, Kazuki Takeda, Tetsuya Yamamoto, Ryusuke Matsukawa and Shinya Kumagai

Department of Electrical and Communication Engineering, Graduate School of Engineering, Tohoku University 6-6-05, Aza-aoba, Aramaki, Aoba-ku, Sendai, Miyagi 980-8579, Japan

ABSTRACT

For the realization of future wireless networks, gigabit wireless technology, which can achieve higher-than-1 Gbps data transmission with extremely low transmit power, is indispensable. We have been studying the distributed antenna network (DAN) and the frequency domain wireless signal processing. In DAN, many antennas or clusters of antennas are spatially distributed over a service area, and they are connected by means of optical fiber links with DAN signal processing center. A number of distributed antennas cooperatively serve mobile users using spatial multiplexing, diversity, array, or relaying technique. In this paper, the recent advances in single-carrier DAN are introduced. Copyright © 2011 John Wiley & Sons, Ltd.

KEYWORDS

component; distributed antenna network; transmit antenna diversity; space–time coding; spatial multiplexing; frequency domain equalization

***Correspondence**

Fumiyuki Adachi, Department of Electrical and Communication Engineering, Graduate School of Engineering, Tohoku University 6-6-05, Aza-aoba, Aramaki, Aoba-ku, Sendai, Miyagi 980-8579, Japan.
E-mail: adachi@ecei.tohoku.ac.jp

1. INTRODUCTION

In the early 1980s, cellular mobile communication systems, which made "anytime, anywhere" communications possible, appeared. Cellular mobile communication systems have evolved from narrowband networks of around 10 kbps (first and second generation systems) to wideband networks of around 10 Mbps (third generation systems). Along with the advancement of wireless techniques, wireless services have been shifted from simple voice to data and then broadband Internet-related data services including video data. Now, the third generation long term evolution systems with 100 Mbps peak data rate are deployed in some countries [1]. A next step is the development of broadband wireless technology that will be used in the fourth generation systems of a peak data rate of around 1 Gbps.

In the future fixed networks, a variety of broadband network services will be made available by the so-called cloud computing networks. Along with this evolution of fixed networks, wireless networks need to further evolve in order to extend a variety of broadband network services available in the fixed networks to wireless users. Wireless access networks need to be enhanced to provide a gigabit wireless pipe to each user mobile terminal (MT).

However, there are a number of important technical issues to be addressed, for example, limited bandwidth, frequency-selective fading, and limited transmit power. In this paper, some of the aforementioned technical issues are discussed, and then a distributed antenna network (DAN) is introduced as a promising solution.

The gigabit wireless channels are extremely frequency selective. The received signal spectrum is severely distorted. An advanced equalization technique is necessary to achieve high-quality gigabit wireless data transmissions in a strong frequency-selective channel. A promising equalization technique is frequency domain equalization (FDE) [2–4]. FDE is an attractive equalization technique that can be combined with transmit diversity, receive diversity, beamforming, multiplexing, cooperative relaying, hybrid automatic repeat request combining, and so on.

In addition, the path loss and shadowing loss cause a severe power loss because the transmit power is limited. The communication range is limited by the uplink

(MT-to-base station (BS)). With the same MT transmit power as in the present wireless systems (i.e., third generation cellular systems), the communication range of the gigabit wireless networks will significantly shrink, and gigabit wireless services may be available near BS only. Therefore, a fundamental change is necessary in wireless access network architecture.

Distributed antenna system or DAN [5] combined with frequency domain signal processing has a potential to solve the aforementioned problems. For uplink signal transmissions, the single-carrier (SC) transmission is promising because it has a lower peak-to-average power ratio than multicarrier transmission (using a transmit power amplifier with the same peak power, SC provides longer communication range than multicarrier). Therefore, we have been investigating the potential of SC-DAN [5].

In this paper, we first give an overview of DAN in Section 2 and then present space–time-coded diversity combined with one-tap FDE for SC-DAN downlink and uplink in Section 3. In Section 4, spatial multiplexing for SC-DAN is presented. Finally, Section 5 offers conclusions.

2. OVERVIEW OF DISTRIBUTED ANTENNA NETWORK

In DAN, as shown in Figure 1, the conventional BS is replaced by the signal processing center (SPC), and many antennas or clusters of antennas are spatially distributed around the SPC so that some antennas can always be visible from an MT with a high probability. Antennas or antenna clusters are connected to an SPC by means of optical fiber links or wireless links. A number of distributed antennas cooperate and act as spatial multiplexing, antenna diversity, relay, or antenna array. Probably the most powerful application is distributed transmit/receive antenna diversity combined with FDE. The problems that result from distance-dependent path loss and shadowing loss as well as from the instantaneous signal power variations due to fading can simultaneously be mitigated.

3. DIVERSITY

For DAN uplink and downlink transmissions, it is desirable to use as many distributed antennas as possible, whereas the number of MT antennas is limited to one or two because there is not enough space to equip too many antennas at an MT. As a promising DAN downlink transmit diversity technique, we have developed a frequency domain space–time block-coded joint transmit/receive diversity (FD-STBC-JTRD) combined with transmit FDE [6]. The FD-STBC-JTRD is an extension of joint transmit diversity/transmit FDE [7] by adding antenna diversity reception and achieves an $N_{\mathrm{dan}} \times N_{\mathrm{mt}}$th order (full) diversity gain, where N_{dan} and N_{mt} represent the number of distributed transmit antennas and that of MT receive antennas, respectively.

The FD-STBC-JTRD allows the use of up to $N_{\mathrm{mt}} = 4$ MT receive antennas while requiring only simple addition, subtraction, and conjugate operations at an MT receiver and thus alleviates the computational complexity problem of MT receivers. Although the number of MT receive antennas is limited to $N_{\mathrm{mt}} = 4$, FD-STBC-JTRD allows the use of an arbitrary number of distributed transmit antennas, N_{dan}. There are two types of transmit FDE weights: minimum mean square error (MMSE) weight and maximum channel capacity weight.

For the uplink transmissions, frequency domain space–time transmit diversity (FD-STTD) [8] is promising. This is because FD-STTD allows the use of an arbitrary number N_{dan} of distributed receive antennas although the number N_{mt} of MT transmit antennas is limited. A combination of FD-STBC-JTRD for downlink and FD-STTD for uplink is suitable for DAN.

In Section 3.1, we present the signal representation for SC-DAN downlink using FD-STBC-JTRD. Section 3.2 introduces the transmit FDE weight for FD-STBC-JTRD. The SC-DAN uplink using FD-STTD is described in Section 3.3. Section 3.4 discusses the computer simulation results. Section 3.5 compares the uplink and downlink performances in terms of bit error rate (BER).

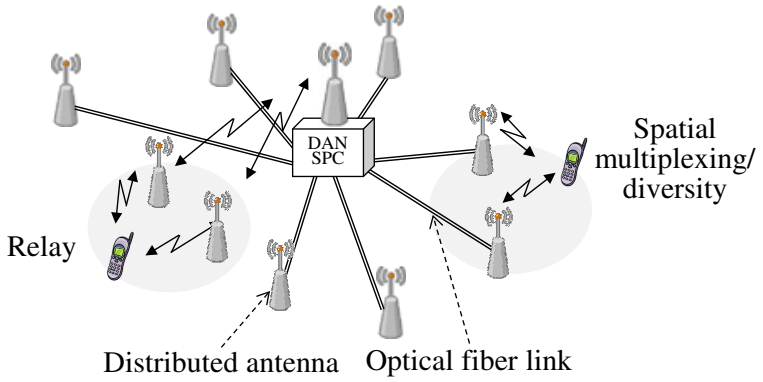

Figure 1. Distributed antenna network (DAN). SPC, signal processing center.

Wirel. Commun. Mob. Comput. 2011; **11**:1551–1563 © 2011 John Wiley & Sons, Ltd.
DOI: 10.1002/wcm

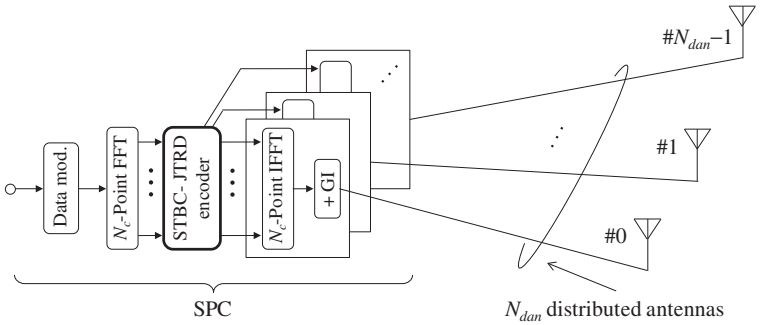

(a) SPC transmitter

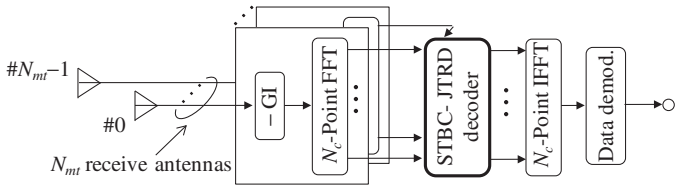

(b) MT receiver

Figure 2. Downlink transmitter/receiver structure using frequency domain space–time block-coded joint transmit/receive diversity (FD-STBC-JTRD): (a) signal processing center (SPC) transmitter and (b) mobile terminal (MT) receiver. FFT, fast Fourier transform; GI, guard interval.

Table I. *J*, *Q*, and coding rate *R*.

No. of transmit antennas	No. of receive antennas	J	Q	Coding rate
Arbitrary	1	1	1	1
	2	2	2	1
	3	3	4	3/4
	4	3	4	3/4

The SC signal transmission is a block transmission. In this paper, a block size of N_c symbols is assumed.

3.1. FD-STBC-JTRD (downlink)

The FD-STBC-JTRD transmitter/receiver structure using N_{dan} distributed transmit antennas and N_{mt} MT receive antennas is illustrated in Figure 2.

At the SPC, a sequence of J blocks of N_c symbols each is transformed by an N_c-point fast Fourier transform (FFT) into a sequence of J frequency domain signals and then encoded into N_{dan} (the number of distributed transmit antennas) streams of Q-coded frequency domain signal blocks each. FD-STBC-JTRD decoding at an MT receiver needs addition, subtraction, and conjugate operations only. A combination of J, Q, and coding rate R are shown in Table I for $N_{\mathrm{mt}} = 1$ to 4.

The achievable diversity gain increases with increasing N_{mt}; however, the coding rate reduces to 3/4 when $N_{\mathrm{mt}} = 3$ and 4. This suggests that the channel capacity or throughput may be maximized at $N_{\mathrm{mt}} = 2$. Later, for the sake of brevity, only the signal representation for $N_{\mathrm{mt}} = 2$ (therefore, $J = Q = 2$) is presented (for $N_{\mathrm{mt}} = 3$ and 4 [6]). However, the computer simulation results on the channel capacity will be shown for $N_{\mathrm{mt}} = 1 \sim 4$ to confirm that $N_{\mathrm{mt}} = 2$ maximizes the channel capacity.

When $N_{\mathrm{mt}} = 2$, a pair of N_c symbol blocks ($J = 2$) to be transmitted are transformed by N_c-point FFT into a pair of frequency domain signals $\{D(k), D_1(k); k = 0 \sim N_c - 1\}$ ($Q = 2$), which is represented by $\mathbf{D}(k) = [D_0(k)\ D_1(k)]^{\mathrm{T}}$. $\mathbf{D}(k)$ is then encoded into N_{dan} pairs of frequency domain-coded signal blocks as

$$\mathbf{S}_{\text{stbc-jtrd}}(k) = \begin{bmatrix} S_{0,0}(k) & S_{1,0}(k) \\ S_{0,1}(k) & S_{1,1}(k) \\ \vdots & \vdots \\ S_{0,N_{\mathrm{dan}}-1}(k) & S_{1,N_{\mathrm{dan}}-1}(k) \end{bmatrix} = \mathbf{W}(k)\mathbf{D}_{\text{stbc-jtrd}}(k) \quad (1)$$

where $S_{qn}(k)$, $q = 0 \sim 1$, is the kth frequency component at the nth transmit antenna. In Equation (1), $\mathbf{D}_{\text{stbc-jtrd}}(k)$ is the encoding matrix of size 2×2 for $N_{\mathrm{mt}} = 2$, given by

$$\mathbf{D}_{\text{stbc-jtrd}}(k) = \begin{bmatrix} D_0(k) & -D_1^*(k) \\ D_1(k) & D_0^*(k) \end{bmatrix} \quad (2)$$

$\mathbf{W}(k)$ is the transmit FDE weight matrix of size $2 \times N_{\text{dan}}$, given as

$$\mathbf{W}(k) = A(k)\mathbf{H}^{\text{H}}(k) \tag{3}$$

where

$$\mathbf{H}(k) = \begin{bmatrix} H_{0,0}(k) & H_{0,1}(k) & \cdots & H_{0,N_{\text{dan}}-1}(k) \\ H_{1,0}(k) & H_{1,1}(k) & \cdots & H_{1,N_{\text{dan}}-1}(k) \end{bmatrix} \tag{4}$$

and $(\,)^{\text{H}}$ denotes the Hermitian transpose. In Equation (3), $A(k)$ is introduced to keep the transmit power intact after the encoding and will be discussed in Section 3.2. $H_{m,n}(k)$ in Equation (4) is the channel gain between the nth distributed transmit antenna and the mth MT receive antenna. An N_c-point inverse FFT (IFFT) is applied to $\{\mathbf{S}(k); k = 0 \sim N_c - 1\}$ to obtain N_{dan} pairs of N_c symbol blocks to be transmitted from N_{dan} distributed antennas.

At the MT receiver, a superposition of N_{dan} pairs of coded N_c symbol blocks is received by $N_{\text{mt}} = 2$ antennas. The received signals are transformed by N_c-point FFT into frequency domain signals, $\{R_{m,0}(k)$ and $R_{m,1}(k); m = 0 \sim 1\}$, which can be expressed using the matrix form as

$$\begin{aligned} \mathbf{R}(k) &= \begin{bmatrix} R_{0.0}(k) & R_{0,1}(k) \\ R_{1.0}(k) & R_{1,1}(k) \end{bmatrix} \\ &= \sqrt{\frac{2E_s}{T_s}}\mathbf{H}(k)\mathbf{S}_{\text{stbc-jtrd}}(k) + \mathbf{N}(k) \end{aligned} \tag{5}$$

where

$$\mathbf{N}(k) = \begin{bmatrix} N_{0,0}(k) & N_{0,1}(k) \\ N_{1,0}(k) & N_{1,1}(k) \end{bmatrix} \tag{6}$$

is the noise matrix with $\{N_{m,q}(k); m = 0 \sim 1, q = 0 \sim 1\}$ being independent zero-mean complex Gaussian variables having variance $2N_0/T_s$, where N_0 denotes the single-sided power spectrum density of additive white Gaussian noise and T_s denotes the data symbol duration.

The FD-STBC-JTRD decoding for $N_{\text{mt}} = 2$ is carried out to obtain the frequency domain signal vector $\hat{\mathbf{D}}(k) = \left[\hat{D}_0(k)\ \hat{D}_1(k)\right]^{\text{T}}$ corresponding to the transmitted signal vector $\mathbf{D}(k) = [D_0(k)D_1(k)]^{\text{T}}$ as

$$\begin{aligned} \hat{\mathbf{D}}(k) &= \begin{bmatrix} R_{0,0}(k) + R^*_{1,1}(k) \\ R_{0,1}(k) - R^*_{1,0}(k) \end{bmatrix} \\ &= \sqrt{\frac{2E_s}{T_s}}A(k)\sum_{m=0}^{1}\sum_{n=0}^{N_{\text{dan}}-1}\left|H_{m,n}(k)\right|^2\mathbf{D}(k) \\ &\quad + \begin{bmatrix} N_{0,0}(k) + N^*_{1,1}(k) \\ N_{0,1}(k) - N^*_{1,0}(k) \end{bmatrix} \end{aligned} \tag{7}$$

Finally, N_c-point inverse FFT is applied to transform $\left\{\hat{\mathbf{D}}(k); k = 0 \sim N_c - 1\right\}$ into a pair of soft decision N_c symbol blocks ($J = 2$).

It can be clearly seen from Equation (7) that the downlink FD-STBC-JTRD using N_{dan} distributed transmit antennas and N_{mt} MT receive antennas can achieve an $N_{\text{dan}} \times N_{\text{mt}}(= 2)$th order (full) diversity gain.

In the following, we consider an SC-DAN with N_{dan} distributed antennas and N_{mt} MT antennas.

3.2. Transmit FDE weight for FD-STBC-JTRD (downlink)

Two types of transmit FDE weights are presented: joint water filling and maximal ratio transmission (WF-MRT) weight [9] and MMSE weight [6].

3.2.1. Joint WF-MRT weight.

The joint WF-MRT weight is the one that maximizes the channel capacity. The problem formulation of channel capacity maximization under the transmit power constraint can be written from Equation (7) as

$$\begin{aligned} \max_{\{A(k)\}} C = \frac{1}{N_c}\sum_{k=0}^{N_c-1}\log_2\Bigg(1 + \frac{E_s}{N_0}\left|A^{\text{wf-mrt}}_{\text{stbc-jtrd}}(k)\right|^2 \\ \left(\sum_{m=0}^{N_{\text{mt}}-1}\sum_{n=0}^{N_{\text{dan}}-1}\left|H_{m,n}(k)\right|^2\right)^2\Bigg) \\ \text{s.t.} \quad \sum_{k=0}^{N_c-1}\Bigg(\left|A^{\text{wf-mrt}}_{\text{stbc-jtrd}}(k)\right|^2\sum_{m=0}^{N_{\text{mt}}-1} \\ \sum_{n=0}^{N_{\text{dan}}-1}\left|H_{m,n}(k)\right|^2\Bigg) = N_c \end{aligned} \tag{8}$$

The solution of Equation (8) is denoted by $\left\{A^{\text{wf-mrt}}_{\text{stbc-jtrd}}(k); k = 0 \sim N_c - 1\right\}$ and is given by

$$\begin{aligned} A^{\text{wf-mrt}}_{\text{stbc-jtrd}}(k) = \frac{1}{\sqrt{\sum_{m=0}^{N_{\text{mt}}-1}\sum_{n=0}^{N_{\text{dan}}-1}\left|H_{m,n}(k)\right|^2}} \\ \times\left[\max\left\{\varphi_{2\text{D}} - \frac{(E_s/2N_0)^{-1}}{\sum_{m=0}^{N_{\text{mt}}-1}\sum_{n=0}^{N_{\text{dan}}-1}\left|H_{m,n}(k)\right|^2}, 0\right\}\right]^{\frac{1}{2}} \end{aligned} \tag{9}$$

where φ_{2D} is set so as to satisfy the transmit power constraint shown in Equation (8). Substituting Equation (9)

into Equation (3) gives the joint WF-MRT weight. The channel capacity C (bps/Hz) for the given channel realization is given as

$$C = \frac{1}{N_c}\sum_{k=0}^{N_c-1}\log_2 \left(1+\frac{E_s}{N_0}\sum_{m=0}^{N_{\mathrm{mt}}-1}\sum_{n=0}^{N_{\mathrm{dan}}-1}\left|H_{m,n}(k)\right|^2 \times \left[\max\left\{\varphi_{2\mathrm{D}}-\frac{(E_s/2N_0)^{-1}}{\sum_{m=0}^{N_{\mathrm{mt}}-1}\sum_{n=0}^{N_{\mathrm{dan}}-1}|H_{m,n}(k)|^2},\,0\right\}\right]\right) \tag{10}$$

3.2.2. MMSE weight.

The MMSE weight is the one that minimizes the mean square error between $\hat{\mathbf{D}}(k) = \left[\hat{D}_0(k)\ \hat{D}_1(k)\right]^{\mathrm{T}}$ and $\mathbf{D}(k) = [D_0(k)\ D_1(k)]^{\mathrm{T}}$. Similar to Equation (8), finding the MMSE weight can be formulated as

$$\min_{\{A(k)\}} e = \sum_{k=0}^{N_c-1}\sum_{m=0}^{N_{\mathrm{mt}}-1} E\left[\left|\hat{D}_m(k)-D_m(k)\right|^2\right] \quad \text{s.t.} \sum_{k=0}^{N_c-1}\left(\left|G\cdot A_{\text{stbc-jtrd}}^{\text{mmse}}(k)\right|^2\sum_{m=0}^{N_{\mathrm{mt}}-1}\sum_{n=0}^{N_{\mathrm{dan}}-1}\left|H_{m,n}(k)\right|^2\right)=N_c \tag{11}$$

With Equation (11) being solved, $\left\{A_{\text{stbc-jtrd}}^{\text{mmse}}(k); k = 0\sim N_c-1\right\}$ is given as [7]

$$A_{\text{stbc-jtrd}}^{\text{mmse}}(k) = \frac{1}{\frac{1}{N_{\mathrm{mt}}}\sum_{m=0}^{N_{\mathrm{mt}}-1}\sum_{n=0}^{N_{\mathrm{dan}}-1}\left|H_{m,n}(k)\right|^2+\left(\frac{E_s}{N_0}\right)^{-1}} \tag{12}$$

and

$$G = \left(\frac{1}{N_c}\sum_{k=0}^{N_c-1}\left\{A_{\text{stbc-jtrd}}^{\text{mmse}}(k)\right\}^2\sum_{m=0}^{N_{\mathrm{mt}}-1}\sum_{n=0}^{N_{\mathrm{dan}}-1}\left|H_{m,n}(k)\right|^2\right)^{-\frac{1}{2}} \tag{13}$$

Substituting Equation (12) into Equation (3) gives the MMSE weight.

3.3. Receive FDE weight for FD-STTD (uplink)

The FD-STBC-JTRD is suitable for the downlink transmission. For the uplink transmission, FD-STTD [8] is suitable because FD-STTD allows the use of an arbitrary number N_{dan} of distributed receive antennas, whereas the number N_{mt} of MT transmit antennas is limited. A pair of N_c symbol block (subscripts "0" and "1" representing even and odd blocks, respectively) are transformed by N_c-point FFT into frequency domain signals represented by $\mathbf{D}(k) = [D_0(k)\ D_1(k)]^{\mathrm{T}}$. The FD-STTD encoding is expressed using the matrix form as [8]

$$\mathbf{D}_{\mathrm{sttd}}(k) = \sqrt{\frac{1}{2}}\begin{pmatrix} D_0(k) & D_1(k) \\ -D_1^*(k) & D_0^*(k)\end{pmatrix} \tag{14}$$

Two pairs of FD-STTD codeword are transmitted from $N_{\mathrm{mt}} = 2$ antennas and are received by N_{dan} distributed antennas, followed by N_c-point FFT. N_{dan} pairs of the received frequency domain signals, $\{R_{n,0}(k)$ and $R_{n,1}(k); n = 0\sim N_{\mathrm{dan}}-1\}$, are expressed using the matrix form as

$$\mathbf{R}_{\mathrm{sttd}}(k) = \begin{bmatrix} R_{0,0}(k) & R_{0,1}(k) \\ R_{1,0}(k) & R_{1,1}(k) \\ \vdots & \vdots \\ R_{N_{\mathrm{dan}}-1,0}(k) & R_{N_{\mathrm{dan}}-1,1}(k)\end{bmatrix} = \sqrt{\frac{2E_s}{T_s}}\mathbf{H}^{\mathrm{T}}(k)\mathbf{D}_{\mathrm{sttd}}(k)+\mathbf{N}(k) \tag{15}$$

where

$$\mathbf{N}(k) = \begin{bmatrix} N_{0,0}(k) & N_{0,1}(k) \\ N_{1,0}(k) & N_{1,1}(k) \\ \vdots & \vdots \\ N_{N_{\mathrm{dan}}-1,0}(k) & N_{N_{\mathrm{dan}}-1,1}(k)\end{bmatrix} \tag{16}$$

is the noise matrix.

After the FD-STTD decoding, the frequency domain signal vector $\hat{\mathbf{D}}(k) = \left[\hat{D}_0(k)\ \hat{D}_1(k)\right]^{\mathrm{T}}$ associated with $\mathbf{D}(k) = [D_0(k)\ D_1(k)]^{\mathrm{T}}$ is obtained as

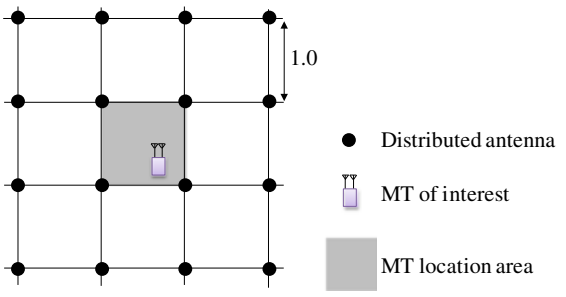

Figure 3. Antenna distribution. MT, mobile terminal.

$$\hat{\mathbf{D}}(k) = \begin{bmatrix} \sum_{n=0}^{N_{\text{dan}}-1} R_{n,0}(k)W^*_{n,0}(k) + \sum_{n=0}^{N_{\text{dan}}-1} R^*_{n,0}(k)W_{n,1}(k) \\ \sum_{n=0}^{N_{\text{dan}}-1} R_{n,0}(k)W^*_{n,1}(k) - \sum_{n=0}^{N_{\text{dan}}-1} R^*_{n,1}(k)W_{n,0}(k) \end{bmatrix}$$
$$= \sqrt{\frac{2E_s}{T_s}} A(k) \sum_{m=0}^{1} \sum_{n=0}^{N_{\text{dan}}-1} \left|H_{m,n}(k)\right|^2 \mathbf{D}(k) \quad (17)$$
$$+ \begin{bmatrix} \sum_{n=0}^{N_{\text{dan}}-1} N_{n,0}(k)W^*_{n,0}(k) + \sum_{n=0}^{N_{\text{dan}}-1} N^*_{n,0}(k)W_{n,1}(k) \\ \sum_{n=0}^{N_{\text{dan}}-1} N_{n,0}(k)W^*_{n,1}(k) - \sum_{n=0}^{N_{\text{dan}}-1} N^*_{n,1}(k)W_{n,0}(k) \end{bmatrix}$$

Similar to the downlink case, the MMSE weight matrix that minimizes the mean square error between $\hat{\mathbf{D}}(k)$ and $\mathbf{D}(k)$ is given, for the case of N_{mt} MT antennas, as [8]

$$\mathbf{W}^{\text{mmse}}_{\text{sttd}}(k) = A^{\text{mmse}}_{\text{sttd}}(k)\mathbf{H}^*(k) = \frac{\mathbf{H}^*(k)}{\frac{1}{N_{\text{mt}}} \sum_{m=0}^{N_{\text{mt}}-1} \sum_{n=0}^{N_{\text{dan}}-1} \left|H_{m,n}(k)\right|^2 + \left(\frac{E_s}{N_0}\right)^{-1}} \quad (18)$$

where

$$A^{\text{mmse}}_{\text{sttd}}(k) = \frac{1}{\frac{1}{N_{\text{mt}}} \sum_{m=0}^{N_{\text{mt}}-1} \sum_{n=0}^{N_{\text{dan}}-1} \left|H_{m,n}(k)\right|^2 + \left(\frac{E_s}{N_0}\right)^{-1}} \quad (19)$$

3.4. Computer simulation results

First, the WF-MRT weight and MMSE weight are compared for SC-DAN downlink using FD-STBC-JTRD. Then, the channel capacity and BER distributions are evaluated for joint WF-MRT weight and with MMSE weight, respectively.

Figure 3 illustrates the DAN antenna distribution. $N = 16$ antennas are uniformly distributed with equal distance between adjacent antennas. An MT having N_{mt} antennas is randomly located in the shaded area. N_{dan} antennas are selected for downlink transmissions, on the basis of the local average received power (i.e., on the basis of the path loss plus shadowing loss). The channel is assumed to follow an $L = 16$-path frequency-selective Rayleigh fading, a log-normally distributed shadowing having standard deviation $\sigma = 7.0$ dB, and a distance-dependent path loss having path loss exponent $\alpha = 3.5$.

3.4.1. Comparison of WF-MRT weight and MMSE weight for SC-DAN downlink using FD-STBC-JTRD.

A comparison between the WF-MRT weight and MMSE weight is made for the case of $N_{\text{dan}} = 4$ and $N_{\text{mt}} = 1$. The normalized transmit E_s/N_0 is set to -10 dB (i.e., the transmit power is the one that provides the received $E_s/N_0 = -10$ dB at the adjacent antenna location).

For both the WF-MRT and MMSE weights, the power allocation is carried out in antenna and frequency dimensions. Figure 4 plots the channel transfer function between transmit antenna 0 and $n(= 0 \sim 3)$ and the squared value of the corresponding transmit FDE weight. Both weights allocate the transmit power across the transmit antennas on the basis of maximal ratio strategy. Therefore, irrespective of the weight, less transmit power is allocated to the transmit antennas in a bad channel condition (Figure 4(a1), 4(a2), 4(b1), and 4(b2)), whereas more transmit power is allocated to the transmit antenna in a good channel condition (Figure 4(a4) and 4(b4)). Power allocation is carried out across the frequencies. In case of the WF-MRT weight, more transmit power is allocated to the frequencies in a good channel condition (Figure 4(b4)).

Figure 5(a) plots the equivalent channel transfer function

$$\hat{H}(k) = \left(\sum_{m=0}^{N_{\text{mt}}-1} \sum_{n=0}^{N_{\text{dan}}-1} \left|H_{m,n}(k)\right|^2 \right)^{\frac{1}{2}}$$

whereas Figure 5(b) plots the squared value of corresponding equivalent transmit FDE weight

$$\left|\hat{W}(k)\right|^2 = \sum_{m=0}^{N_{\text{mt}}-1} \sum_{n=0}^{N_{\text{dan}}-1} \left|W_{m,n}(k)\right|^2$$

It can be seen from Figure 5(b) that joint WF-MRT weight allocates more transmit power to the frequencies in a better channel condition (some frequencies in a bad channel condition are not used at all). On the other hand, the MMSE weight uses the frequencies even in a poor condition.

3.4.2. FD-STBC-JTRD with joint WF-MRT weight.

Figure 6 plots the 1% outage capacity of SC-DAN downlink using FD-STBC-JTRD with joint WF-MRT weight, below which the channel capacity falls with 1% probability, for the normalized transmit $E_s/N_0 = 10$ dB. The use of $N_{\text{mt}} = 2$ maximizes the channel capacity. This is a consequence of the trade-off between diversity gain and coding rate; as N_{mt} increases, the diversity gain increases, but the coding rate R reduces to 3/4 when $N_{\text{mt}} = 3$ (Table I).

Figure 7 plots the required transmit E_s/N_0 for a 1% outage capacity of 5 bps/Hz as a function of N_{dan} for the case of $N_{\text{mt}} = 2$. Increasing N_{dan} reduces the required transmit E_s/N_0. The required E_s/N_0 reduction by increasing N_{dan} from 1 to 6 is about 5.6 dB.

3.4.3. FD-STBC-JTRD with joint MMSE weight.

The BER performance of SC-DAN downlink using FD-STBC-JTRD with MMSE weight is also evaluated. Figure 8 plots the required transmit E_s/N_0 for a 1% outage BER of 10^{-4} as a function of N_{dan} when $N_{\text{mt}} = 2$. Increasing N_{dan} reduces the required transmit E_s/N_0. The required E_s/N_0 reduction by increasing N_{dan} from 1 to 6 is about 6.5 dB.

3.5. Uplink/downlink performance comparison

The BER performances are compared assuming FD-STBC-JTRD using joint MMSE weight for the uplink

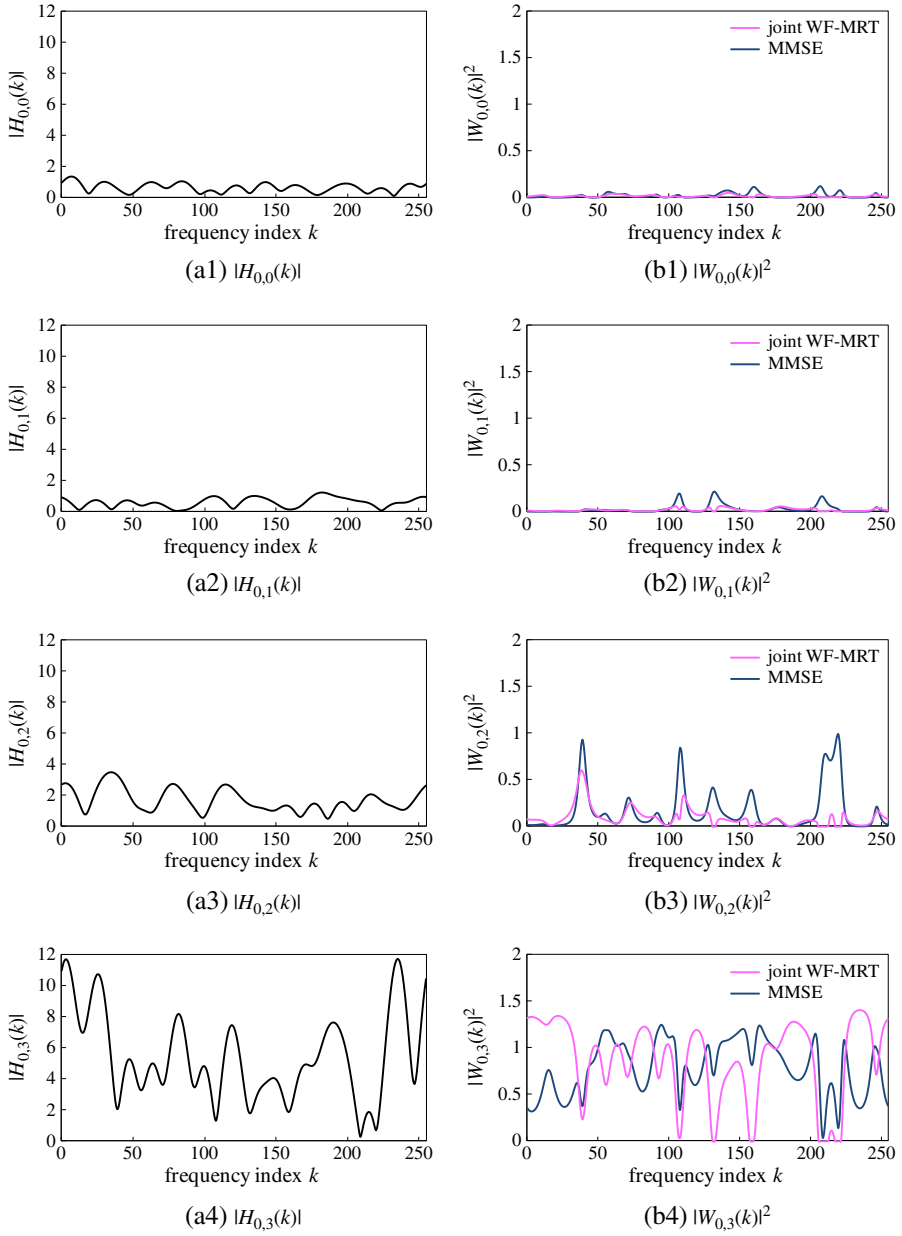

Figure 4. Channel transfer function and squared value of frequency domain equalization weight when $N_{\text{mt}} = 1$ and $N_{\text{dan}} = 4$: (a1) $|H_{0,0}(k)|$, (a2) $|H_{0,1}(k)|$, (a3) $|H_{0,2}(k)|$, (a4) $|H_{0,3}(k)|$, (b1) $|W_{0,0}(k)|^2$, (b2) $|W_{0,1}(k)|^2$, (b3) $|W_{0,2}(k)|^2$, and (b4) $|W_{0,3}(k)|^2$. WF-MRT, water filling and maximal ratio transmission; MMSE, minimum mean square error.

and FD-STTD using MMSE weight for the downlink. N_{dan} arbitrary distributed antennas and $N_{\mathrm{mt}} = 2$ MT antennas are assumed. The same antenna distribution pattern as in Section 3.4 is assumed.

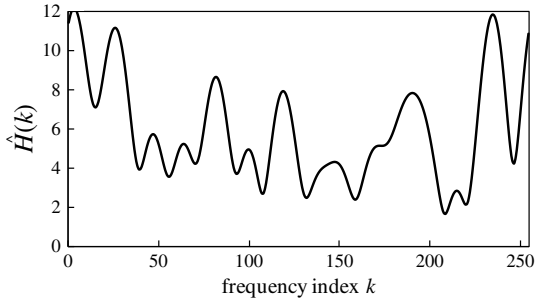

(a) $\hat{H}(k)$

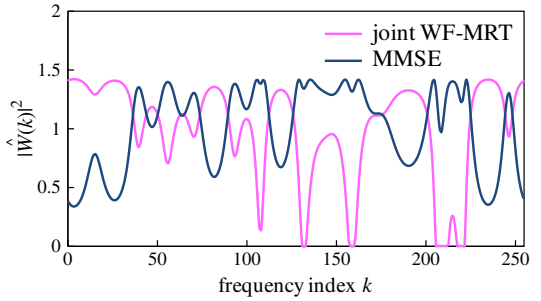

(b) $|\hat{W}(k)|^2$

Figure 5. Equivalent channel transfer function and squared value of equivalent transmit frequency domain equalization weight when $N_{\mathrm{mt}} = 1$ and $N_{\mathrm{dan}} = 4$: (a) $|\hat{H}(k)|$ and (b) $|\hat{W}(k)|^2$. WF-MRT, water filling and maximal ratio transmission; MMSE, minimum mean square error.

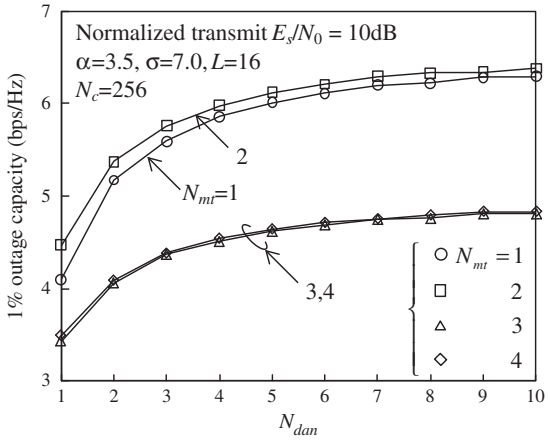

Figure 6. 1% outage channel capacity of single-carrier distributed antenna network downlink using frequency domain space–time block-coded joint transmit/receive diversity with joint water filling and maximal ratio transmission weight.

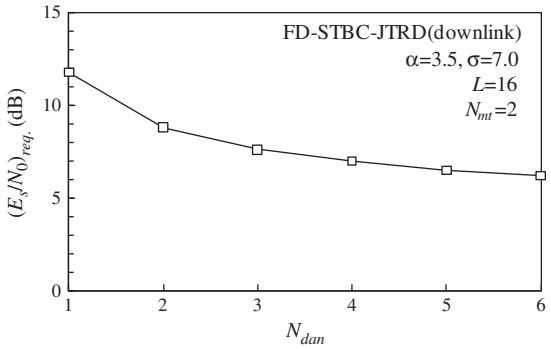

Figure 7. Required transmit E_s/N_0 for a 1% outage capacity of 5 bps/Hz. FD-STBC-JTRD, frequency domain space-time block-coded joint transmit/receive diversity.

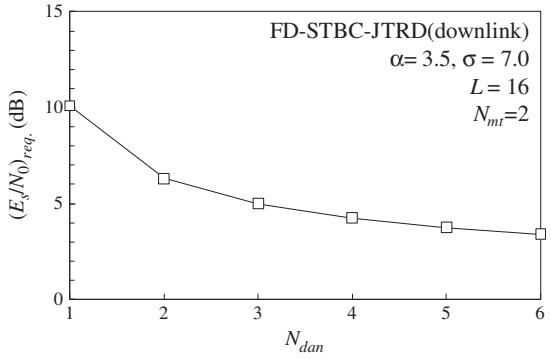

Figure 8. Required transmit E_s/N_0 for a 1% outage bit error rate of 10^{-4}. FD-STBC-JTRD, frequency domain space–time block-coded joint transmit/receive diversity.

The complementary cumulative distribution function of the measured downlink and uplink BERs are plotted in Figure 9 for the normalized transmit $E_s/N_0 = 5$ dB. It can be clearly seen from the figure that well-balanced downlink and uplink transmissions can be achieved. By increasing N_{dan} (the number of distributed transmit/receive antennas), the probability that the received signal power drops due to path loss, shadowing loss, and frequency-selective fading can be more reduced and hence the BER can be significantly reduced.

4. SPATIAL MULTIPLEXING

The spatial multiplexing is an attractive technique to achieve highly spectrum-efficient transmission [10]. Multiple distributed antennas in DAN can be also used not only for space diversity but also for the spatial multiplexing to improve the throughput of the systems [11]. Here, we consider the uplink case using N_{mt} transmit antennas and N_{dan} receive distributed antennas (N_{dan} receive antennas are selected among N distributed antennas).

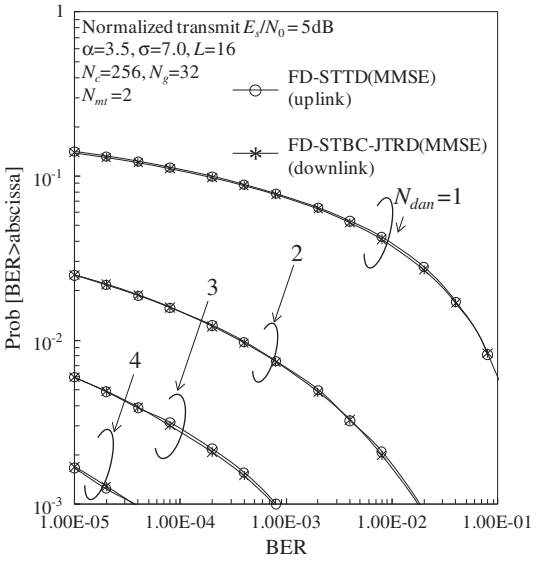

Figure 9. Uplink/downlink performance comparison. BER, bit error rate; FD-STTD, frequency domain space–time transmit diversity; FD-STBC-JTRD, frequency domain space–time block-coded joint transmit/receive diversity; MMSE, minimum mean square error.

4.1. Signal detection for spatial multiplexing

Recently, we proposed a maximum likelihood detection (MLD) employing QR decomposition and M-algorithm (QRM-MLD) [12] for the SC spatial multiplexing in a frequency-selective fading channel [13]. The SC frequency domain maximum likelihood block signal detection employing QR decomposition and M-algorithm (QRM-MLBD) is a powerful signal detection scheme combined with FDE. The receiver structure of SC frequency domain QRM-MLBD for a cyclic prefix (CP)-inserted SC (CP-SC) spatial multiplexing is illustrated in Figure 10.

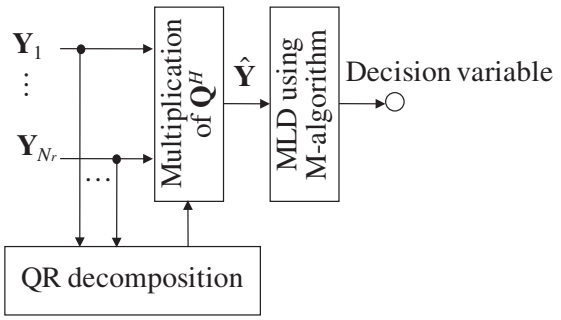

Figure 10. Single-carrier frequency domain maximum likelihood block signal detection employing QR decomposition and M-algorithm. MLD, maximum likelihood detection.

Assuming the $N_{\mathrm{mt}} \times N_{\mathrm{dan}}$ spatial multiplexing, the frequency domain received signal vector at the nth receive distributed antenna $\mathbf{Y}_n = [Y_n(0), \ldots, Y_n(k), \ldots, Y_n(N_c - 1)]^{\mathrm{T}}$ is expressed as

$$\mathbf{Y}_n = \sqrt{\frac{2E_s}{T_s}} \sum_{m=1}^{N_{\mathrm{mt}}} \mathbf{H}_{n,m}\mathbf{F}\mathbf{d}_m + \mathbf{N}_n \tag{20}$$

where $\mathbf{F}$ is the discrete Fourier transform matrix of size $N_c \times N_c$, $\mathbf{H}_{n,m} = \mathrm{diag}[H_{n,m}(0), \ldots, H_{n,m}(k), \ldots, H_{n,m}(N_c - 1)]$ is the frequency domain channel matrix between the mth transmit antenna and nth receive antenna, and $\mathbf{N}_n = [N_n(0), \ldots, N_n(k), \ldots, N_n(N_c - 1)]^{\mathrm{T}}$ is the frequency domain noise vector. From Equation (20), the $N_{\mathrm{dan}}N_c \times 1$ overall frequency domain received signal $\mathbf{Y}$ is given by

$$\begin{aligned}
\mathbf{Y} &= \left[\{\mathbf{Y}_1\}^{\mathrm{T}} \quad \cdots \quad \{\mathbf{Y}_{N_{\mathrm{dan}}}\}^{\mathrm{T}} \right]^{\mathrm{T}} \\
&= \sqrt{\frac{2E_s}{T_s}} \begin{bmatrix} \mathbf{H}_{1,1}\mathbf{F} & \mathbf{H}_{1,2}\mathbf{F} & \cdots & \mathbf{H}_{1,N_{\mathrm{mt}}}\mathbf{F} \\ \mathbf{H}_{2,1}\mathbf{F} & \mathbf{H}_{2,2}\mathbf{F} & \cdots & \mathbf{H}_{2,N_{\mathrm{mt}}}\mathbf{F} \\ \vdots & \vdots & \ddots & \vdots \\ \mathbf{H}_{N_{\mathrm{dan}},1}\mathbf{F} & \mathbf{H}_{N_{\mathrm{dan}},2}\mathbf{F} & \cdots & \mathbf{H}_{N_{\mathrm{dan}},N_{\mathrm{mt}}}\mathbf{F} \end{bmatrix} \\
&\quad \times \begin{bmatrix} \mathbf{d}_1 \\ \vdots \\ \mathbf{d}_{N_{\mathrm{mt}}} \end{bmatrix} + \begin{bmatrix} \mathbf{N}_1 \\ \vdots \\ \mathbf{N}_{N_{\mathrm{dan}}} \end{bmatrix} \\
&= \sqrt{\frac{2E_s}{T_s}} \mathbf{H} \begin{bmatrix} \mathbf{d}_1 \\ \vdots \\ \mathbf{d}_{N_{\mathrm{mt}}} \end{bmatrix} + \mathbf{N}
\end{aligned} \tag{21}$$

where $\mathbf{H}$ is an equivalent channel matrix of size $N_{\mathrm{dan}}N_c \times N_{\mathrm{mt}}N_c$. QRM-MLBD can be applied to the SC spatial multiplexing by treating a concatenation of the space and frequency domain channel and discrete Fourier transform as this equivalent channel.

The QRM-MLBD consists of two steps: QR decomposition and M-algorithm. First, the QR decomposition is applied to the equivalent channel matrix $\mathbf{H}$ to obtain $\mathbf{H} = \mathbf{QR}$, where $\mathbf{Q}$ is an $N_{\mathrm{dan}}N_c \times N_{\mathrm{mt}}N_c$ unitary matrix and $\mathbf{R}$ is an $N_{\mathrm{mt}}N_c \times N_{\mathrm{mt}}N_c$ upper triangular matrix. The transformed frequency domain received signal $\hat{\mathbf{Y}} = \left[\hat{Y}(0), \ldots, \hat{Y}(k), \ldots, \hat{Y}(N_{\mathrm{mt}}N_c - 1)\right]^{\mathrm{T}}$ is obtained as

$$\hat{\mathbf{Y}} = \mathbf{Q}^H\mathbf{Y} = \sqrt{\frac{2E_s}{T_s}}\mathbf{R} \begin{bmatrix} \mathbf{d}_1 \\ \vdots \\ \mathbf{d}_{N_{\mathrm{mt}}} \end{bmatrix} + \mathbf{Q}^H\mathbf{N} \tag{22}$$

It can be understood from Equation (22) that the MLD can be converted to the successive tree search problem and that the computational complexity can be reduced by introducing the M-algorithm into the successive tree search. SC frequency domain QRM-MLBD can achieve the BER performance close to the MLD with significantly reduced computational complexity compared with the MLD.

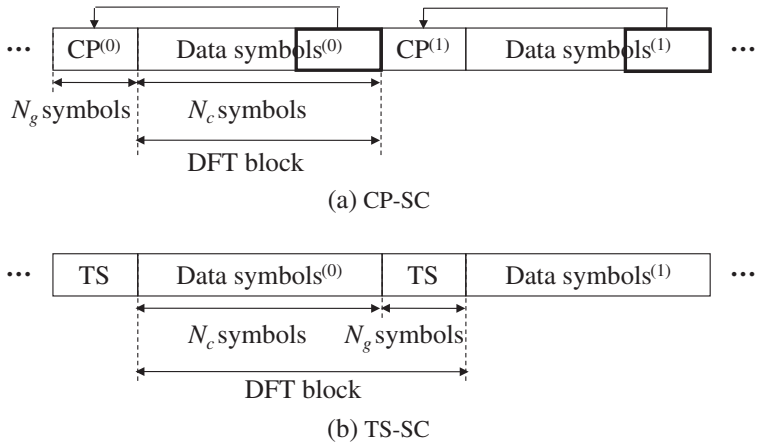

Figure 11. (a) Cyclic prefix inserted single carrier (CP-SC) and (b) training sequence-aided single carrier (TS-SC). DFT, discrete Fourier transform.

However, the CP-SC block transmission requires a fairly large number of surviving paths in the M-algorithm; therefore, its computational complexity is still very high. To overcome this problem, we suggested using a known training sequence (TS)-aided SC (TS-SC) transmissions, in which the known TS in the previous block acts as the CP in the present block, as shown in Figure 11 [14],[15]. The known TS is exploited in the M-algorithm to reduce the number of surviving paths.

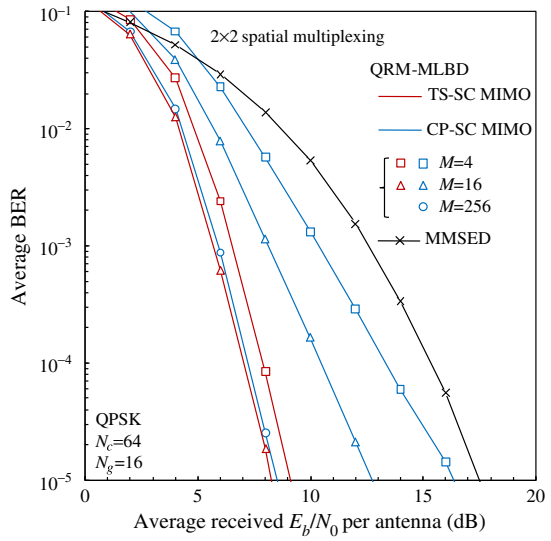

Figure 12. Bit error rate (BER) performance comparison between cyclic prefix-inserted single carrier (CP-SC) and training sequence-aided single carrier (TS-SC). QPSK, quadrature phase shift keying; QRM-MLBD, maximum likelihood block signal detection employing QR decomposition and M-algorithm; MIMO, multiple input multiple output; MMSED, minimum mean square error detection.

4.2. Computer simulation results

First, we compare CP-SC and TS-SC for point-to-point transmission using 2×2 spatial multiplexing. We assume a block transmission of $N_c = 64$ symbols. The channel is assumed to be a symbol-spaced $L = 16$-path frequency-selective block Rayleigh fading channel having uniform power delay profile. Ideal channel estimation is assumed. The average BER performance of SC frequency domain QRM-MLBD is plotted in Figure 12. Also plotted is the BER performance achievable by MMSE detection. As the number M of surviving paths in the M-algorithm increases, the BER performance improves. When TS-SC is used, the required number of surviving paths in the M-algorithm is greatly reduced while achieving almost the same BER performance as CP-SC.

In DAN, seven antennas are distributed over an entire cell to compare with the conventional cellular network as illustrated in Figure 13. Figure 14 plots the complementary cumulative distribution function of the computer-simulated BER when $N_{\mathrm{mt}} = N_{\mathrm{dan}} = 2$. The single-user and single-cell uplink SC-DAN is considered. The normalized transmit E_s/N_0 is set to 10 dB (i.e., the transmit power is the

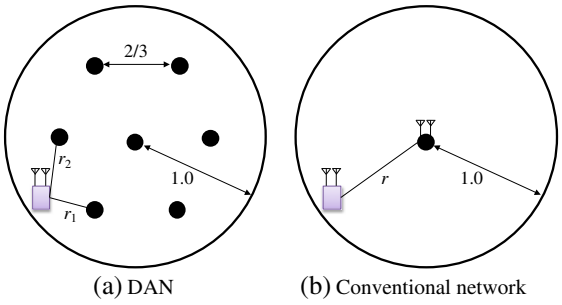

Figure 13. System model: (a) distributed antenna network (DAN) and (b) conventional network. $N_{\mathrm{mt}} = N_{\mathrm{dan}} = 2$.

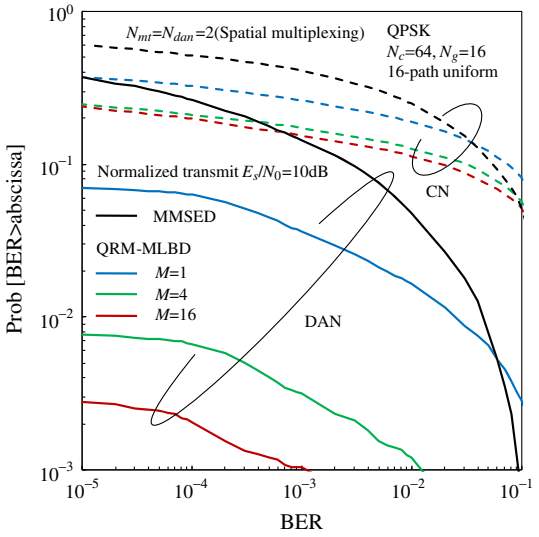

Figure 14. Complementary cumulative distribution function of bit error rate (BER). $N_{\mathrm{mt}} = N_{\mathrm{dan}} = 2$. QPSK, quadrature phase shift keying; MMSED, minimum mean square error detection; QRM-MLBD, maximum likelihood block signal detection employing QR decomposition and M-algorithm; CN, conventional network; DAN, distributed antenna network.

one that provides the received $E_s/N_0 = 10$ dB at the cell edge). MT transmits N_{mt} parallel data streams by using spatial multiplexing. It is assumed that N_{dan} distributed antennas nearest from the MT are selected as receive antennas. It can be seen that DAN can significantly reduce the BER compared with the conventional network. When QRM-MLBD with $M = 16$ is used, DAN can reduce the outage probability by 20% compared with the conventional network (the outage probability is defined as the probability that the BER exceeds the required $BER = 10^{-3}$ in this paper). Furthermore, QRM-MLBD can reduce the BER compared with the MMSE signal detection. The performance improvement is significant in DAN.

5. CONCLUSION

Distributed antenna network is a promising wireless technology to realize gigabit wireless data transmissions. In this paper, we have introduced gigabit DAN combined with SC frequency domain signal processing. Distributed transmit/received diversity can solve the problems arising from severe channel selectivity and limited transmit power. It is desirable to use as many distributed antennas as possible to achieve higher diversity gain while limiting the number of MT antennas to one or two so as to alleviate the complexity problem of MT. It was shown that the balanced downlink/uplink performance can be achieved by using FD-STBC-JTRD for the downlink and FD-STTD for the uplink. We also presented a spatial multiplexing using TS-SC and QRM-MLBD to improve the transmission performance compared with the MMSE spatial filtering.

REFERENCES

1. Astély D, Dahlman E, Furuskär A, Jading Y, Lindström M, Parkvall S. LTE: the evolution of mobile broadband. *IEEE Communications Magazine* 2009; **47**(4): 44–51.
2. Falconer D, Ariyavistakul SL, Benyamin-Seeyar A, Eidson B. Frequency domain equalization for single-carrier broadband wireless systems. *IEEE Communications Magazine* 2002; **40**(4): 58–66.
3. Adachi F, Sao T, Itagaki T. Performance of multicode DS-CDMA using frequency domain equalization in a frequency selective fading channel. *IEE Electronics Letters* 2003; **39**(2): 239–241.
4. Adachi F, Garg D, Takaoka S, Takeda K. Broadband CDMA techniques. *IEEE Wireless Communications Magazine* 2005; **12**(2): 8–18.
5. Adachi F, Takeda K, Obara T, Yamamoto T. Recent advances in single-carrier frequency-domain equalization and distributed antenna network. *IEICE Transactions on Fundamentals* 2010; **E93-A**(11): 2201–2211.
6. Tomeba H, Adachi F. Frequency-domain space-time block coded-joint transmit/receive diversity for the single carrier transmission, In *Proceedings of the 10th IEEE International Conference on Communication Systems (ICCS2006)*, Singapore, 2006.
7. Choi RL, Murch RD. Frequncy domain pre-equalization with transmit diversity for MISO broadband wireless communications, In *Proceedings of the IEEE Vehicular Technology Conference (VTC2002-Fall)*, Vancouver, Canada, 2002.
8. Takeda K, Itagaki T, Adachi F. Application of space-time transmit diversity to single-carrier transmission with frequency-domain equalization and receive antenna diversity in a frequency-selective fading channel. *IEE Proceedings-Communications* 2004; **151**(6): 627–632.
9. Matsuda H, Matsukawa R, Obara T, Takeda K, Adachi F. Channel capacity of distributed antenna network using space-time block coded-joint transmit/receive diversity, In *Proceedings of 12th IEEE International Conference on Communication Systems (ICCS 2010)*, Singapore, 2010.
10. Foschini GJ, Gans MJ. On limit of wireless communications in a fading environment when using multiple antennas. *Wireless Personal Communications* 1998; **6**(3): 311–335.

11. Saleh A, Rustako A, Roman R. Distributed antennas for indoor radio communications. *IEEE Transactions on Communications* 1987; **35**(12): 1245–1251.
12. Kim LJ, Yue J. Joint channel estimation and data detection algorithms for MIMO-OFDM systems, In *Proceedings of the 36th Asilomar Conference on Signals, System and Computers*, 2002; 1857–1861.
13. Nagatomi K, Higuchi K, Kawai H. Complexity reduced MLD based on QR decomposition in OFDM MIMO multiplexing with frequency domain spreading and code multiplexing, In *Proceedings of the IEEE Wireless Communications and Networking Conference (WCNC 2009)*, 2009; 1–6.
14. Yamamoto T, Takeda K, Adachi F. Training sequence-aided single-carrier block signal detection using QRM-MLD, In *Proceedings of the IEEE Wireless Communications & Networking Conference 2010 (WCNC 2010)*, Sydney, Australia, 2010.
15. Yamamoto T, Takeda K, Adachi F. Training sequence-aided QRM-MLD block signal detection for single-carrier MIMO spatial multiplexing, In *Proceedings of the IEEE International Conference on Communications (ICC 2011)*, Kyoto, Japan, 2011.

AUTHORS' BIOGRAPHIES

Fumiyuki Adachi received B.S. and Dr. Eng. degrees in Electrical Engineering from Tohoku University, Sendai, Japan, in 1973 and 1984, respectively. In April 1973, he joined the Electrical Communications Laboratories of Nippon Telegraph & Telephone Corporation (now NTT) and conducted various types of research related to digital cellular mobile communications. From July 1992 to December 1999, he was with NTT Mobile Communications Network, Inc. (now NTT DoCoMo, Inc.), where he led a research group on wideband/broadband CDMA wireless access for IMT-2000 and beyond. Since January 2000, he has been with Tohoku University, Sendai, Japan, where he is a Professor of Electrical and Communication Engineering at the Graduate School of Engineering. He was appointed as a Distinguished Professor in 2011.

His research interests are in CDMA wireless access techniques, equalization, transmit/receive antenna diversity, MIMO, adaptive transmission, and channel coding, with particular application to broadband wireless communications systems. He is a program leader of the 5-year Global COE Program "Center of Education and Research for Information Electronics Systems" (2007-2011), awarded by the Ministry of Education, Culture, Sports, Science and Technology of Japan. From October 1984 to September 1985, he was a United Kingdom SERC Visiting Research Fellow in the Department of Electrical Engineering and Electronics at Liverpool University. He is an IEICE Fellow and was a co-recipient of the IEICE Transactions Best Paper of the Year Award 1996, 1998, and 2009 and also a recipient of the Achievement Award 2003. He is an IEEE Fellow and was a co-recipient of the IEEE Vehicular Technology Transactions Best Paper of the Year Award 1980 and again 1990 and also a recipient of the Avant Garde Award 2000. He was a recipient of Thomson Scientific Research Front Award 2004, Ericsson Telecommunications Award 2008, Telecom System Technology Award 2009, and Prime Minister Invention Prize 2010.

Kazuki Takeda received his B.S., M.S., and Dr. Eng. degrees in Communications Engineering from Tohoku University, Sendai, Japan, in 2006, 2008, and 2010, respectively. From April 2008 to March 2011, he was a Japan Society for the Promotion of Science (JSPS) Research Fellow. Since April 2011, he has been with Panasonic Corporation. He was a recipient of the 2009 IEICE RCS (Radio Communication Systems) Active Research Award.

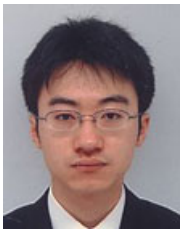

Tetsuya Yamamoto received his B.S. degree in Electrical, Information and Physics Engineering in 2008 and M.S. degree in Communications Engineering in 2010 from Tohoku University, Sendai, Japan. Currently, he is a Japan Society for the Promotion of Science (JSPS) Research Fellow, studying toward his Ph.D. degree at the Department of Electrical and Communications Engineering, Graduate School of Engineering, Tohoku University. His research interests include frequency-domain equalization and signal detection techniques for mobile communication systems. He was a recipient of the 2008 IEICE RCS (Radio Communication Systems) Active Research Award.

Ryusuke Matsukawa received his B.S. degree in Electrical, Information and Physics Engineering from Tohoku University, Sendai, Japan, in 2010. Currently, he is a graduate student at the Department of Electrical and Communications Engineering, Graduate School of Engineering, Tohoku University. His research interests include distributed antenna networks and multiple antenna techniques.

Shinya Kumagai received his B.S. degree in Information and Intelligent Systems from Tohoku University, Sendai, Japan, in 2011. Currently, he is a graduate student at the Department of Electrical and Communication Engineering, Tohoku University. His research interests include distributed MIMO diversity and multiplexing techniques for mobile communication systems.